

Transport in quasiperiodic interacting systems: from superdiffusion to subdiffusion

Yevgeny Bar Lev,¹ Dante M. Kennes,² Christian Klöckner,³ David R. Reichman,¹ and Christoph Karrasch³

¹*Department of Chemistry, Columbia University,
3000 Broadway, New York, New York 10027, USA**

²*Department of Physics, Columbia University, 3000 Broadway, New York, New York 10027, USA*

³*Dahlem Center for Complex Quantum Systems and Fachbereich Physik,
Freie Universität Berlin, 14195 Berlin, Germany*

Using a combination of numerically exact and renormalization-group techniques we study the nonequilibrium transport of electrons in an one-dimensional interacting system subject to a quasiperiodic potential. For this purpose we calculate the growth of the mean-square displacement as well as the melting of domain walls. While the system is nonintegrable for all studied parameters, there is no *finite region* of parameters for which we observe diffusive transport. In particular, our model shows a rich dynamical behavior crossing over from superdiffusion to subdiffusion. We discuss the implications of our results for the general problem of many-body localization, with a particular emphasis on the rare region Griffiths picture of subdiffusion.

Introduction. — The finite energy transport properties of quantum-mechanical systems generally fall into one of the three standard categories: ballistic, diffusive, and the complete absence of transport altogether. Ballistic transport is only possible in special, so-called integrable cases (such as free fermions) where an extensive set of local conserved quantities prevents currents from scattering. Interacting, clean systems are generically diffusive, while the cessation of transport is a hallmark of systems that completely fail to equilibrate, such as those that undergo Anderson localization [1]. The study of the transition between such regimes has been energized by the recent focus on systems that undergo many-body localization (MBL) [2–4]. In the standard quenched disordered variants of such systems, dynamical behavior is observed that exhibits a rich set of distinct transport behaviors [5–9]. Interacting quasiperiodic (QP) systems are also believed to exhibit similar behavior, and are the basis for several recent experimental studies on MBL [10, 11]. Unfortunately, very little is known about transport in such systems. Here, we fill this vital gap via a finite-temperature version [12–14] of the time-dependent matrix renormalization group (tDMRG) [15, 16] as well as the functional renormalization group (FRG) [17, 18].

Model. — We consider a one-dimensional model of spinless fermions, subject to a quasiperiodic potential (QP),

$$\hat{H} = \sum_{m=1}^{L-1} [J (\hat{c}_m^\dagger \hat{c}_{m+1} + \text{h.c.}) + U \hat{n}_m \hat{n}_{m+1}] + \sum_{m=1}^L V_m \hat{n}_m, \quad (1)$$

which using the Jordan-Wigner transformation exactly maps to XXZ spin model [20]. Here L is the length of the system, \hat{c}_m^\dagger (\hat{c}_m) create (annihilate) a spinless fermion on site m , “h.c.” denotes Hermitian conjugate, \hat{n}_m is the corresponding density, J is the hopping rate, which without the loss of generality we set to $J = 1$, U is the

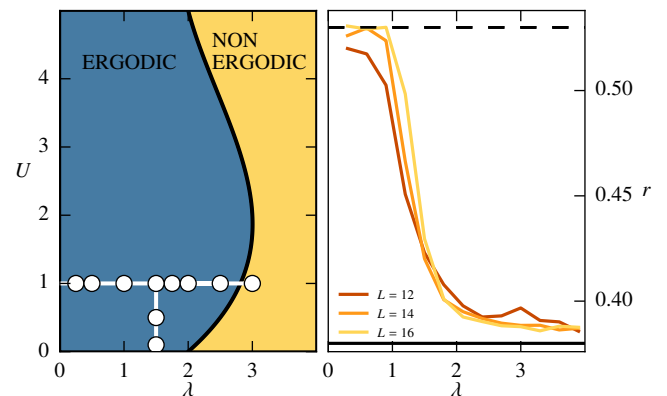


Figure 1. (Left) A schematic phase diagram (U, λ) of the system (c.f. Fig. 19 in Ref. [19]). The white circles represent the points studied in this work. (Right) The average gap ratio r in the middle of the spectrum for various strengths of the QP potential, $U = 1$, and different system sizes (lighter shades represent larger system sizes). The dashed black line corresponds to the Wigner-Dyson limit and the solid black line to the Poisson limit.

interaction strength and V_m is a QP potential of the form,

$$V_m = \lambda \cos(2\pi\delta m + \phi), \quad (2)$$

where δ is an irrational number which we will take to be inverse of the golden mean, $\delta = (\sqrt{5} - 1)/2$ and ϕ is a random phase. For $U = 0$, this model reduces to the Aubry-André model, which has a transition between all localized and all extended single-particle states which occurs at $\lambda/J = 2$ [21]. For $\lambda > 2J$ transport is absent in this model, while for $\lambda < 2J$ transport is ballistic [22]. For $\lambda = 0$ the Hamiltonian is integrable even in the presence of interactions ($U \geq 0$). For $U < 2$ one can construct quasilocal conserved quantities to demonstrate that transport is ballistic [23, 24], while for $U > 2$ transport is diffusive [25–28]. When both λ and U are nonzero the system is nonintegrable, and has been studied numerically and experimentally. It has a MBL transition which

at infinite temperatures occurs for $\lambda/J > 2$ [10, 29, 30]. We are interested to study transport in regimes of weak integrability, in the limits where the transport in the integrable limit is ballistic. Therefore through this work we use $U \leq 2$ (see left panel of Fig. 1, for the parameters we use). We would also like to avoid the MBL phase where an emergent integrability appears [31–36]. For this purpose we search for the *approximate* location of the MBL transition in this model by calculating the gap ratio $r_n = \max(\delta_n/\delta_{n+1}, \delta_{n+1}/\delta_n)$ in the middle of the spectrum, where δ_n are the eigenvalue differences. The gap ratio is a convenient metric of short-range correlations in the eigenvalues’ statistics which was introduced in Ref. [37]. Ergodicity is assumed when the obtained probability distribution of r_n (or the unfolded δ_n) matches the one of the corresponding random matrix ensemble [38]. In Fig. 1 we calculate the mean value of r_n averaged over 1000 realization of the random phase in (2) and 50 values of r_n computed in the middle of the many-body spectrum. We repeat this analysis for $U = 1$, a few system sizes, and various amplitudes of the QP potential, and infer the location of the transition from the crossing point between the different curves. Similarly to previous studies [39], the crossing point drifts to larger values of λ when the system size is increased, indicating that the transition occurs for $\lambda > 2$. This value is consistent with previous studies (c.f. Fig. 19 in Ref. [19], but note a factor of 2 difference in the definition of the kinetic energy). Since we endeavor in this work *not* to calculate the *precise* location of the transition (which is quite difficult to do, given the small system sizes which are accessible) but to merely obtain the values of λ for which the system is clearly within the ergodic phase we focus mostly on $\lambda \lesssim 3$, although the extent of the ergodic phase might be somewhat larger.

To characterize the transport we use a combination of a numerically exact method, tDMRG and an approximate method, FRG, which allows us to access significantly larger system sizes and longer times [40]. We evaluate the infinite temperature density-density correlation function,

$$C_{i,j}(t) = 2^{-L} \text{Tr} \left(\hat{n}_i^z(t) - \frac{1}{2} \right) \left(\hat{n}_j^z - \frac{1}{2} \right), \quad (3)$$

and calculate the analog of the mean-square displacement (MSD),

$$x^2(t) = \frac{1}{L} \sum_{i,j=1}^L (i-j)^2 C_{i,j}(t). \quad (4)$$

Normally the MSD scales as power-law with time, $x^2 \sim t^\alpha$, where α is the dynamical exponent. For systems with ballistic transport, $\alpha = 2$, and for diffusive systems $\alpha = 1$. Systems with no transport or transport with a MSD growing more slowly than any power law will have $\alpha = 0$.

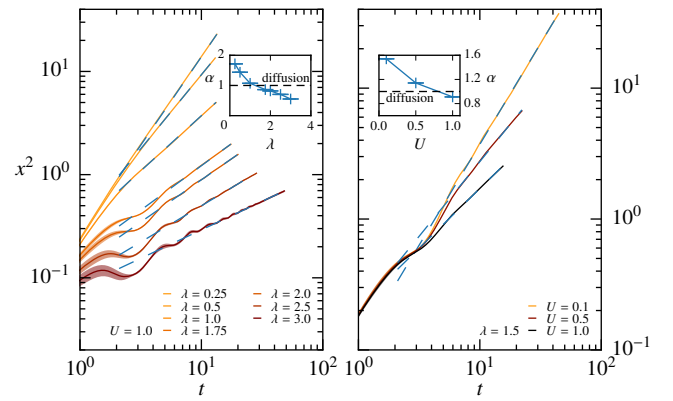


Figure 2. Mean-square displacement as a function of time on a log-log scale, for various amplitudes of the QP potential. The left panel shows the horizontal cut through the phase diagram at Fig. 1, and the right panel shows the vertical cut. Darker colors represent larger parameters, and the width of the lines represent the statistical error bars. Blue dashed lines show the quality of the power-law fits, and the insets present the corresponding dynamical exponents. The system size used is $L = 100$.

To reduce the effects of the boundaries we use systems of sizes $L = 100 - 200$.

Superdiffusive regime. — We start by analyzing the vicinity of the integrable limits $U = 0$ and $\lambda = 0$. In both cases, we do not observe a sharp crossover from ballistic to diffusive behavior but uncover an extended *superdiffusive regime* where the MSD growth as a power law in time, $x^2 \sim t^\alpha$, with an exponent $1 < \alpha < 2$. This is illustrated in the left (right) panels of Fig. 2 for the horizontal (vertical) cuts through the phase diagram (see Fig. 1). The occurrence of superdiffusive transport in the presence of interactions and disorder is in striking contrast to the behavior of clean systems where integrability breaking terms normally lead to diffusion (for spin systems, see Refs. [41–44]). However, a simple estimate of the mean free time of scattering from the external potential gives a time-scale of $\tau \sim 1/\lambda^2$, which is about $\tau \approx 16$ for the smallest λ we study and is comparable to our maximal simulation times. Therefore while we convincingly observe superdiffusion over one decade in time, we cannot rule out the scenario where it is merely a transient phenomenon. Simulating for longer times is exponentially hard within tDMRG since while it is a numerically exact method, the accessible time scales are bounded by the growth of entanglement entropy. Therefore to substantiate our observation of superdiffusion, we complement the tDMRG simulation by a different approach which can reach to much longer times at the price of being approximate. Since transport in the system is characterized by power laws it is natural to use a renormalization-group based method for this purpose.

Domain wall dynamics. — In order to access longer time scales and larger system sizes we use the functional

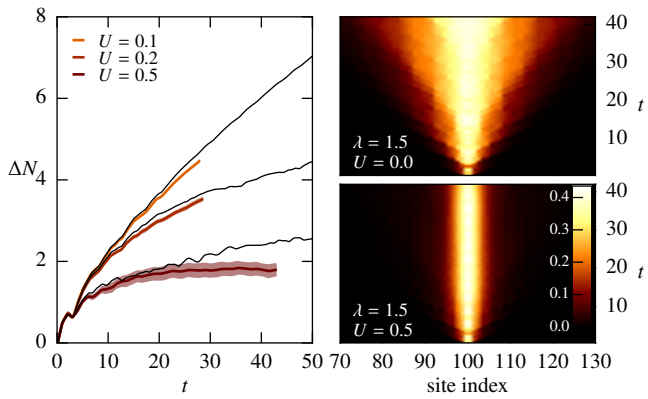


Figure 3. Mass transport for a domain wall initial condition. The right side shows the mass difference, $|n_i(t) - n_i(0)|$, as a function of time for two values of the interaction $U = 0$ and 0.5 , and demonstrates that transport, which is ballistic at $U = 0$, becomes successively suppressed when switching on interactions. The left side compares tDMRG (colored lines) and FRG (black lines) results for the total mass transferred to the left side as a function of time, for fixed λ and varying U . The width of the colored lines represent the statistical error.

renormalization group (FRG) [17, 18] implemented on the real-time Keldysh contour [45–47]. The FRG provides an *a priori* exact reformulation of a quantum many-body problem in terms of flow equations for vertex functions with an infrared cutoff as the flow parameter [40]. We truncate these equations to leading order, which renders the framework approximate with respect to the interaction strength. Due to its RG nature, the FRG can capture power laws, and the corresponding exponents can be computed up to the linear order in the interaction strength, U (all higher-order contributions are uncontrolled). The computational effort of the FRG calculation is not sensitive to the build up of entanglement in the system, and scales linearly with time. In one dimension one can access times of $t \sim 1000$ for systems of up to $L \sim 1000$ sites. Since the MSD is a two-body correlation function, it cannot be computed reliably using a first-order FRG scheme. To circumvent this issue we investigate transport via a different protocol which can be simulated both by the FRG and the tDMRG: the melting of domain walls.

Domain wall dynamics provide a natural sensor for MBL physics [48] that can be realized straightforwardly in cold-atom experiments [49]. To be precise, we prepare the system in a state where all sites on the left (right) are occupied (empty) and compute the number of particles ΔN spreading between these two regions. In the localized phase, the melting of the domain wall is suppressed, while in the ergodic phase it is characterized by a power law growth of the transported number of particles, $\Delta N \sim t^{\alpha/2}$, with the same exponent α , as the MSD (if calculated for the *same* initial conditions). We now

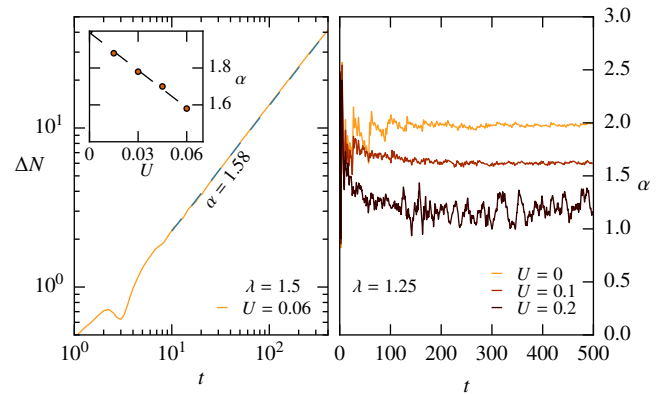


Figure 4. (Left) Log-log plot of the transported number of particles ΔN as a function of time. The blue dashed line is a linear fit to the data from which the dynamical exponent is extracted, and the inset shows the dynamical exponent as computed from FRG for various interaction strengths, $\lambda = 1.5$. (Right) Log-derivative of the ΔN as function of time, $\lambda = 1.25$.

study the ergodic phase close to integrability. Since FRG is exact in the limit of $U = 0$, we focus on the vertical cut through the phase diagram in Fig. 1. In the absence of interactions, ΔN grows linearly with time indicating ballistic transport (see right panel of Fig. 3). Finite $U > 0$ leads to slower transport, and the FRG data is in good agreement with the accurate reference provided by the tDMRG on intermediate time scales (see left panel of Fig. 3). The FRG can now be used to push the calculation to significantly larger times, and a superdiffusive power law with $1 < \alpha < 2$ can be identified unambiguously (see left panel of Fig. 4). Since in this setup we use small interactions it is important to work with times longer than the mean-free time of scattering between two particles, $\tau_{ee} \sim 1/U^2$, otherwise a transient ballistic transport would be observed. Not only the transport we observe is always sub-ballistic, but in our simulations we also use times which are about 2-20 times longer than the scattering mean-free time $\tau_{ee} \sim 25 - 277$. To verify that the extracted dynamical exponents do not drift with time we also compute the log-derivative ($d \log \Delta N / d \log t$) and observe that it saturates to a plateau (see right panel of Fig 4), which indicates that the calculated dynamical exponents are asymptotic within the FRG scheme. It is also important to check that the extracted dynamical exponent α scales linearly with U , which is self-consistent with the assumptions of FRG (see inset of Fig. 4).

In the vicinity of $U = 0$, the dynamical exponents agree qualitatively with those governing the growth of the MSD (see Fig. 2). A strict quantitative comparison is however not possible since we did not find a parameter set for which the exponents can be determined reliably in *both* setups. e.g., at $\lambda = 1.5$, $U = 0.1$ (see Fig. 2), the domain-wall exponent is no longer in the purely lin-

ear regime, and the higher-order corrections cannot be computed reliably by the FRG. More importantly, there is no general reason to expect that the exponents governing the spreading of the domain wall and the MSD, computed for an infinite temperature initial condition, should coincide: the former is a far out-of-equilibrium initial condition while the latter describes linear response. The difference between both setups becomes particularly apparent at larger $U \sim 0.5$ where we can no longer unambiguously identify power laws in the evolution of the domain wall but observe a strong suppression of transport. Since this effect appears to be a specific hallmark of the (domain wall) initial conditions and does not directly coalesce with the focus of this work, we leave the exploration of this interesting regime to future work. We have thus provided evidence that transport close of the integrable (ballistic) limits of vanishing interactions or disorder is superdiffusive. We will now demonstrate that subdiffusion materializes for larger amplitudes of the QP potential.

Subdiffusive regime. — For interacting one-dimensional systems subject to an uncorrelated disordered potential, transport is surprisingly subdiffusive [5–7] (see also recent reviews [8, 9] and references within). It has been proposed that subdiffusion is a result of rare spatial regions with anomalously large escape times (which for example could correspond to areas with very short local localization lengths) [7, 9, 50, 51]. These rare regions dramatically affect transport in one dimension, since every particle has to pass through all effective barriers. This picture, dubbed the *Griffiths picture*, does not generically apply when there are long correlations in the underlying disorder potential, in particular in the case where the potential is QP [50, 51]. The Griffiths picture thus should predict diffusion for QP potentials [50].

On the left panel of Fig. 2 we present the MSD as a function of time for various strengths of the QP potential and $U = 1$. The computation was carried out at infinite temperature (cf. Eq. (3)). From the inset, which shows the extracted dynamical exponent, it is clear that there is actually no *finite* regime of parameters for which the system is diffusive. Similar behavior was observed in an experimental and numerical study, which appeared while this work was in preparation [11]. To verify that the observed behavior occurs also for *pure* initial states, we calculated the MSD and the entanglement entropy (EE) starting from the Néel state (see Fig. 5). We note that for the system we study the Néel state is a state with relatively high energy density, lying close to the center of the many-body band, and has been successfully utilized to demonstrate MBL in cold atoms experiments [10, 11]. However unlike the experiments, we do *not* allow volatility in the initial state, namely we have exactly one particle sitting on every other lattice site. Similarly to the infinite temperature initial state, for the Néel state initial condition both the MSD and the EE show power law

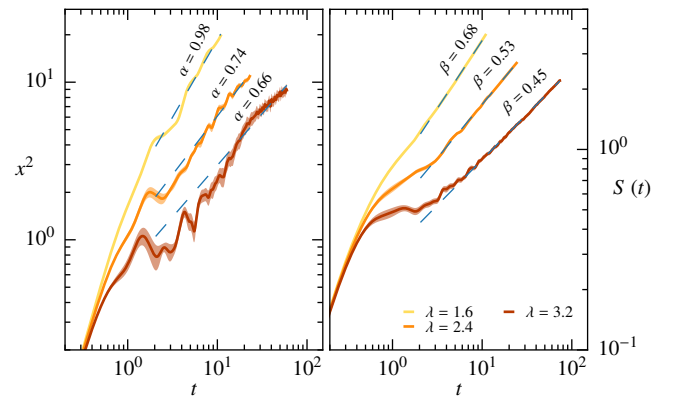


Figure 5. Mean-square displacement (left) and entanglement entropy (right) on a log-log scale as a function of time for the Néel state as the initial state. Parameters used: $L = 100$, interaction strength $U = 2$ and $\lambda = 1.6, 2.4$ and 3.2 (darker colors designate higher values). Dashed lines represent linear fits used to extract the dynamical exponents. Diffusion corresponds to, $\alpha = \beta = 1$.

growth with time with dynamical exponents which depend on the amplitude of the QP potential (EE was also studied in Ref. [30]). We note that while for the Néel state initial condition the growth of the MSD appears to be subdiffusive for the simulated times the extraction of the exponent is extremely unreliable due to presence of oscillations in the data, *which do not disappear with better averaging*. This precludes from making meaningful comparison between the dynamical exponent of the EE (β) with the dynamical exponent of the MSD (α). For a comparison of such exponents in disordered systems the interested reader is referred to Ref. [8].

Discussion. — In this Letter we have demonstrated that a simple but generic one dimensional interacting system with a quasiperiodic potential exhibits an unexpectedly rich dynamical behavior, exhibiting a crossover from superdiffusive to subdiffusive transport. Within the study of systems connected to the problem of many-body localization, the discovery of superdiffusive behavior is a new one. While superdiffusion is expected to exist on *finite* time scales asymptotically close to an integrable point, our finding that it also holds for substantial interaction and amplitude strengths is surprising.

We have also presented numerical evidence which is inconsistent with the prevailing explanation for subdiffusion in MBL systems, namely the Griffiths picture [7, 9, 50, 51]. The Griffiths picture naturally relies on the presence of uncorrelated quenched disorder in the system, which is crucial for generating a sufficient density of rare blocking inclusions. Therefore for systems with uncorrelated disorder in dimensions greater than one, those with strongly correlated disorder, or for the quasiperiodic case studied here, the Griffiths picture should yield asymptotic diffusive transport. Contrary to these predictions

we observe subdiffusive spin transport and a sublinear spreading of entanglement entropy. We note that while our numerical results are valid only for relatively short time scales, there is no *a priori* reason why subdiffusive behavior should manifest within the Griffiths picture on any time scale in the quasiperiodic case studied here. Our results are in line with a very recent experimental study, which appeared while our work was in preparation [11]. There it was argued that while rare regions cannot be a result of the quasiperiodic potential, they may follow from rare spatial regions in the initial state [11]. We stress that the infinite temperature state, which we use as the initial state here, is clearly translationally invariant, but still exhibits subdiffusion. Moreover we have verified that subdiffusion is robust also when a *pure* initial state without any special spatial structure is taken (here we considered the experimentally relevant Néel state).

Given our results, we speculate that subdiffusion is a result of atypical *transition rates* between the eigenstates of the *noninteracting* Hamiltonian and not necessary atypical *spatial regions*. We order the eigenstates of the noninteracting Hamiltonian according to their energies and define the transition rates between any two states, α and β to be given by its Golden rule value, $W_{\alpha\beta} = |V_{\alpha\beta}|^2 / (E_\alpha - E_\beta)$, where $V_{\alpha\beta}$ are the matrix elements of the Hamiltonian terms which couple α and β . This picture is akin to phenomenological trap models of glassy systems in configurational space [52]. In particular, these models posit a “particle,” representing a location in parameter or phase space, which hops on a random energy landscape and with broadly distributed waiting times. Indeed given a master equation of the form

$$\frac{dP_n}{dt} = W_{n,n-1}(P_{n-1} - P_n) + W_{n,n+1}(P_{n+1} - P_n), \quad (5)$$

with a distribution of hopping times $p(W) \sim W^{-\alpha}$, then subdiffusion with an exponent that smoothly decreases and vanishes at a well-defined transition, as well as all of the scaling relations normally associated with the Griffiths picture of MBL, are naturally obtained [8, 53]. It is important to emphasize that the process we consider is not associated with the classical exploration of a complex energy landscape by activation processes through contact with the environment, but instead the transitions are induced internally. Indeed, a recent calculation of the dynamics of Anderson localization on the Bethe lattice, long believed to be a proxy for MBL in low space dimensions, shows subdiffusive behavior strikingly similar to that observed near the MBL transition and comports with the trap-like model picture presented above [54].

We would like to stress that while there is an apparent similarity between the mechanism we propose and the Griffiths picture, in the case of our mechanism the dependence on the dimensionality of the physical system is quite weak, since any d -dimensional system is mapped

effectively to a model with no spatial structure. Moreover there is no direct connection between the waiting time within a “trap” in the configurational space and *spatially* atypical regions. Therefore unlike the Griffiths scenario, our picture allows for subdiffusion in higher dimensions as well as in the presence of long range spatial correlations in the potential. Some evidence for subdiffusion in two dimensions exists within the framework of self-consistent many-body dynamics [55]. The microscopic mechanism of these atypical transition rates, as well as a rigorous mapping to a quantum trap-like model as envisioned above, have yet to be obtained and are certainly goals worthy of future work.

YB and DRR acknowledge funding from the Simons Foundation (#454951, David R. Reichman). We acknowledge support by the Deutsche Forschungsgemeinschaft through the Emmy Noether program KA 3360/2-1 (CKI and CKa), as well as through DK 2115/1-1 (D.K.). Part of the simulations in this work were performed using computing resources granted by RWTH Aachen University under project rwth0013 and rwth0057. YB, DK and CKI contributed equally to this work.

* yevgeny.barlev@columbia.edu

- [1] P. W. Anderson, *Phys. Rev.* **109**, 1492 (1958)
- [2] D. Basko, I. L. Aleiner, and B. L. Altshuler, *Ann. Phys. (N. Y.)*. **321**, 1126 (2006)
- [3] E. Altman and R. Vosk, *Annu. Rev. Condens. Matter Phys.* **6**, 383 (2015)
- [4] R. Nandkishore and D. A. Huse, *Annu. Rev. Condens. Matter Phys.* **6**, 15 (2015)
- [5] Y. Bar Lev and D. R. Reichman, *Phys. Rev. B* **89**, 220201 (2014)
- [6] Y. Bar Lev, G. Cohen, and D. R. Reichman, *Phys. Rev. Lett.* **114**, 100601 (2015)
- [7] K. Agarwal, S. Gopalakrishnan, M. Knap, M. Müller, and E. Demler, *Phys. Rev. Lett.* **114**, 160401 (2015)
- [8] D. J. Luitz and Y. Bar Lev, (2016), arXiv:1610.08993
- [9] K. Agarwal, E. Altman, E. Demler, S. Gopalakrishnan, D. A. Huse, and M. Knap, *Ann. Phys.*, 1600326 (2017)
- [10] M. Schreiber, S. S. Hodgman, P. Bordia, H. P. Lüschen, M. H. Fischer, R. Vosk, E. Altman, U. Schneider, and I. Bloch, *Science* **349**, 842 (2015)
- [11] H. P. Lüschen, P. Bordia, S. Scherg, F. Alet, E. Altman, U. Schneider, and I. Bloch, (2016), arXiv:1612.07173
- [12] C. Karrasch, J. H. Bardarson, and J. E. Moore, *Phys. Rev. Lett.* **108**, 227206 (2012)
- [13] T. Barthel, *New J. Phys.* **15**, 073010 (2013)
- [14] D. M. Kennes and C. Karrasch, *Comput. Phys. Commun.* **200**, 37 (2016)
- [15] S. R. White, *Phys. Rev. Lett.* **69**, 2863 (1992)
- [16] U. Schollwöck, *Ann. Phys. (N. Y.)*. **326**, 96 (2011)
- [17] M. Salmhofer, *Renormalization* (Springer Berlin Heidelberg, Berlin, Heidelberg, 1999)
- [18] W. Metzner, M. Salmhofer, C. Honerkamp, V. Meden, and K. Schönhammer, *Rev. Mod. Phys.* **84**, 299 (2012)
- [19] S. Bera, T. Martyneec, H. Schomerus, F. Heidrich-

- Meisner, and J. H. Bardarson, , 1 (2016), [arXiv:1611.01687](#)
- [20] P. Jordan and E. Wigner, *Z. Phys.* **47**, 631 (1928)
- [21] S. Aubry and G. André, *Ann. Isr. Phys. Soc* **3**, 18 (1980)
- [22] H. Hiramoto and M. Kohmoto, *Phys. Rev. Lett.* **62**, 2714 (1989)
- [23] T. Prosen, *Phys. Rev. Lett.* **106**, 217206 (2011)
- [24] E. Ilievski and J. De Nardis, “On the Microscopic Origin of Ideal Conductivity,” (2017), [arXiv:1702.02930](#)
- [25] X. Zotos and P. Prelovšek, *Phys. Rev. B* **53**, 983 (1996)
- [26] R. Steinigeweg and W. Brenig, *Phys. Rev. Lett.* **107**, 250602 (2011)
- [27] M. Žnidarič, *Phys. Rev. Lett.* **106**, 220601 (2011)
- [28] C. Karrasch, J. E. Moore, and F. Heidrich-Meisner, *Phys. Rev. B* **89**, 075139 (2014)
- [29] S. Iyer, V. Oganesyan, G. Refael, and D. A. Huse, *Phys. Rev. B* **87**, 134202 (2013)
- [30] T. Roscilde, P. Naldesi, and E. Ercolessi, *SciPost Phys.* **1**, 010 (2016)
- [31] D. A. Huse, R. Nandkishore, and V. Oganesyan, *Phys. Rev. B* **90**, 174202 (2014)
- [32] M. Serbyn, Z. Papić, and D. A. Abanin, *Phys. Rev. Lett.* **111**, 127201 (2013)
- [33] V. Ros, M. Müller, and A. Scardicchio, *Nucl. Phys. B* **891**, 420 (2015)
- [34] J. Z. Imbrie, *J. Stat. Phys.* **163**, 998 (2016)
- [35] J. Z. Imbrie, *Phys. Rev. Lett.* **117**, 027201 (2016)
- [36] J. Z. Imbrie, V. Ros, and A. Scardicchio, (2016), [arXiv:1609.08076](#)
- [37] V. Oganesyan, A. Pal, and D. A. Huse, *Phys. Rev. B* **80**, 115104 (2009)
- [38] Y. Y. Atas, E. Bogomolny, O. Giraud, and G. Roux, *Phys. Rev. Lett.* **110**, 084101 (2013)
- [39] V. Oganesyan and D. A. Huse, *Phys. Rev. B* **75**, 155111 (2007)
- [40] “See supplemental material at [url] for details on the numerical procedure used in this work.”
- [41] P. Jung, R. W. Helmes, and A. Rosch, *Phys. Rev. Lett.* **96**, 067202 (2006)
- [42] X. Zotos, *Phys. Rev. Lett.* **92**, 067202 (2004)
- [43] R. Steinigeweg, F. Heidrich-Meisner, J. Gemmer, K. Michielsen, and H. De Raedt, *Phys. Rev. B* **90**, 094417 (2014)
- [44] C. Karrasch, D. M. Kennes, and F. Heidrich-Meisner, *Phys. Rev. B* **91**, 115130 (2015)
- [45] S. G. Jakobs, V. Meden, and H. Schoeller, *Phys. Rev. Lett.* **99**, 150603 (2007)
- [46] D. M. Kennes, S. G. Jakobs, C. Karrasch, and V. Meden, *Phys. Rev. B* **85**, 085113 (2012)
- [47] D. M. Kennes and V. Meden, *Phys. Rev. B* **88**, 165131 (2013)
- [48] J. Hauschild, F. Heidrich-Meisner, and F. Pollmann, *Phys. Rev. B* **94**, 161109 (2016)
- [49] J.-y. Choi, S. Hild, J. Zeiher, P. Schauss, A. Rubio-Abadal, T. Yefsah, V. Khemani, D. A. Huse, I. Bloch, and C. Gross, *Science* **352**, 1547 (2016)
- [50] S. Gopalakrishnan, M. Müller, V. Khemani, M. Knap, E. A. Demler, and D. A. Huse, *Phys. Rev. B* **92**, 104202 (2015)
- [51] S. Gopalakrishnan, K. Agarwal, E. A. Demler, D. A. Huse, and M. Knap, *Phys. Rev. B* **93**, 134206 (2016)
- [52] C. Monthus and J.-P. Bouchaud, *J. Phys. A: Math. Gen.* **29**, 3847 (1996)
- [53] S. Alexander, J. Bernasconi, W. R. Schneider, and R. Orbach, *Rev. Mod. Phys.* **53**, 175 (1981)
- [54] G. Biroli and M. Tarzia, (2017)
- [55] Y. Bar Lev and D. R. Reichman, *EPL* **113**, 46001 (2016)